Original Article

Apatinib enhances the antitumor effects of radiation in HeLa cell line mouse model of invasive cervical cancer

Yun Wang[1#], Li Zhang[1#], Wei Liu[2#], Jing-Pin Yang[3], Hong-Ju Peng[4], Jian-Wen Zhang[1,5,6]

[1]Department of Oncology, the Affiliated Hospital of Southwest Medical University, Luzhou, China; [2]Department of Oncology, People's Hospital of Dazu District, Chongqing, China; [3]Department of Oncology, the First Hospital of Guangyuan, Guangyuan, China; [4]Department of Oncology, Second People's Hospital of Neijiang, Neijiang, China; [5]Nuclear Medicine and Molecular Imaging Key Laboratory of Sichuan Province, Luzhou, China; [6]Academician (Expert) Workstation of Sichuan Province, Luzhou, China

Contributions: (I) Conception and design: W Liu, JW Zhang; (II) Administrative support: JP Yang, HJ Peng; (III) Provision of study materials or patients: Y Wang, L Zhang, W Liu; (IV) Collection and assembly of data: Y Wang, L Zhang, W Liu; (V) Data analysis and interpretation: JW Zhang; (VI) Manuscript writing: All authors; (VII) Final approval of manuscript: All authors.

[#]These authors contributed equally to this work.

Correspondence to: Jian-Wen Zhang. Department of Oncology, the Affiliated Hospital of Southwest Medical University, 25 Taiping Road, Luzhou 646000, China. Email: zhangjianwen66@126.com.

Background: There is the lack of reports on apatinib (APA) combined with radiation in the treatment of cervical cancer. The aim of our study was to investigate the anti-tumor effect of APA combined with radiation using an *in vivo* model of cervical cancer.

Methods: The mouse models, established using Henrietta Lacks (HeLa) cells, were randomly divided into 4 groups: the control group, radiotherapy (RT) alone group, cisplatin (DDPs) combination RT group (DDPs + RT), and APA combination RT group (APA + RT). The expressions of the vascular endothelial growth factor receptor-2 (VEGFR-2), platelet endothelial cell adhesion molecule-1 (CD31), proliferating cell nuclear antigen (Ki-67), and histone H2AX family member (γ-H2AX) were determined using immunohistochemistry (IHC), the extent of apoptosis was determined using terminal deoxynucleotidyl transferase (TdT)-mediated (dUTP) nick-end labeling (TUNEL), and tumor metabolism was determined using micro18F-fluorodexyglucose positron emission tomography/computed tomography. The length of survival was observed and recorded.

Results: The positive expressions of VEGFR-2, CD31, and Ki-67 in the APA + RT group were obviously reduced compared with the control, RT, and DDPs + RT groups ($P<0.05$). The positive expression of γ-H2AX was obviously increased compared with the control and RT groups ($P<0.05$), whereas the apoptosis rate in the APA + RT group was obviously increased compared with the control, RT, and DDPs + RT groups ($P<0.05$). The tumor metabolism and volume in the APA + RT group were obviously reduced compared with the control, RT, and DDPs + RT groups. The length of survival was prolonged by 22 and 11 days in the APA + RT group compared with the RT and DDPs + RT groups, respectively ($P<0.05$).

Conclusions: The combination of APA and RT could significantly enhance the anti-tumor efficacy of RT and prolong the median survival in a mouse model of cervical cancer.

Keywords: Antiangiogenic therapy; apatinib (APA); cervical cancer; cisplatin (DDP); radiotherapy (RT)

Submitted Feb 14, 2022. Accepted for publication Apr 07, 2022.
doi: 10.21037/atm-22-1442
View this article at: https://dx.doi.org/10.21037/atm-22-1442

Introduction

Cervical cancer is a common malignant tumor among women worldwide. More than half a million women are diagnosed with cervical cancer every year and over 300,000 deaths are attributed to cervical cancer worldwide. Approximately 90% of cervical cancers cases occur in low- and middle-income countries (1). The incidence rate of cervical cancer is 13.9 per 100,000 (2). In 2018, cervical cancer ranked fourth among women in terms of morbidity and mortality (3). China, a developing country, has a high incidence of cervical cancer. In 2020, according to the China cancer statistics study, the incidence and mortality of cervical cancer in China ranked sixth and seventh amongst all tumors for women (4).

According to the International Federation of Gynecology and Obstetrics (FIGO, 2018) staging system, 37.2% of patients are diagnosed at locally advanced stages (5,6). The overall prognosis of locally advanced cervical cancer remains poor, and even among patients with early cervical cancer, in comparison with stage IB1, the death rate of patients in stage IB2 cervical cancer is nearly triple (7). Stage III cervical cancer is characterized by an even less favorable 5-year survival rate (40.7% in stage IIIA, 41.4% in stage IIIB, and 37.5% in stage IIIC) (8).

Surgery and radiotherapy (RT) are common treatments for cervical cancer. RT, particularly concurrent RT based on cisplatin (DDPs), is a standard treatment for locally advanced cervical cancer. However, it is associated with severe side effects and poor tolerance by patients. The incidence of gastrointestinal toxicity is higher at stages 3 and above (9). Non-cisplatin-based concurrent chemo RT is also associated with a high incidence of toxicity and side effects (34.4%) (10). Antiangiogenic drugs, including bevacizumab, combined with RT, can improve the overall survival (OS) rate in patients with cervical cancer (1).

Apatinib (APA) is a novel oral tyrosine kinase inhibitor that is associated with low toxicity. The main therapeutic target of APA is vascular endothelial growth factor receptor-2 (VEGFR-2). There has been wide administration of APA to patients with gastric cancer, hepatocellular carcinoma, lung cancer, and prostate cancer, and it has been found to be associated with improved efficacy and safety (11-14). In cervical cancer, APA is primarily used in combination with chemotherapy among patients with recurrent cancer (15,16). However, there is a lack of research on the use of APA as a combination treatment with RT in cervical cancer, and the mechanisms including the effects on VEGFR-2, platelet endothelial cell adhesion molecule-1 (CD31), proliferating cell nuclear antigen (Ki-67), and histone H2AX family member (γ-H2AX) are not clear. Herein, we investigated the anti-tumor effect and mechanism of APA in combination with RT to provide evidence for the use of APA combined with RT as a treatment for advanced cervical cancer in a clinical setting. We present the following article in accordance with the ARRIVE reporting checklist (available at https://atm.amegroups.com/article/view/10.21037/atm-22-1442/rc).

Methods

Experimental design

Establishment of tumor-bearing mouse models

Henrietta Lacks (HeLa) cells, a cervical cancer cell line, were obtained from the Oncology Department of Affiliated Hospital of Southwest Medical University. The HeLa cells were stored at –80 ℃ in a refrigerator, thawed in a water bath at 37 ℃, and centrifuged at 1,000 rpm for 1 minute. The supernatant was discarded, 1.0 mL of the medium was added to the frozen storage tube, and the cell sediment at the bottom of the tube was mixed to obtain a uniform cell suspension. Subsequently, the cell suspension was transferred into a 25 cm^2 culture bottle and 3 mL of medium was added, followed by incubation at a constant temperature of 37 ℃ in an atmosphere of 5% CO_2. Cell growth was observed daily using phase-contrast microscopy and the medium was changed every 2 days.

When in the exponential growth phase, HeLa cells (5×10^6/mL) were inoculated subcutaneously in the root of the right hind limb in healthy BALB-C female nude mice (n=48; 4–5 weeks; 18–20 g weight; Chongqing Tianxinhuafu Biotechnology Company, China; Certificate No. 2014-004) after disinfecting the skin with 75% medical-grade alcohol. Specific-pathogen-free (SPF) feeding was carried out at the medical laboratory animal center. Daily changes in mental, dietary, weight, and behavioral patterns, as well as tumor volume, were recorded. Experiments were conducted when the volume of the transplanted tumor was approximately 100–150 mm^3. A protocol was prepared before the study without registration. Experiments were performed under a project license (No. swum20210388) granted by the Institutional Animal Care and Treatment Committee of Southwest Medical University, in compliance with China national guidelines for the care and use of animals.

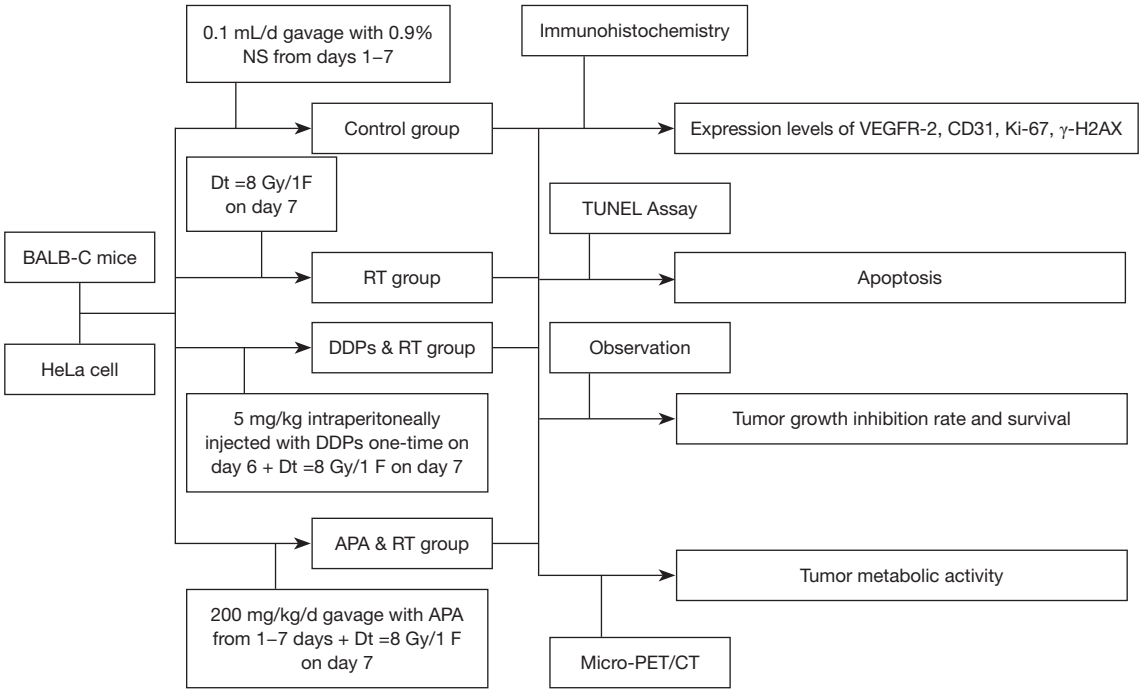

Figure 1 Research design and route. NS, normal saline; RT, radiotherapy; DDPs, cisplatin; APA, apatinib; VEGFR-2, vascular endothelial growth factor receptor-2; CD31, platelet endothelial cell adhesion molecule-1; Ki-67, proliferating cell nuclear antigen; γ-H2AX, histone H2AX family member; TUNEL, TdT-mediated dUTP Nick-End Labeling apoptosis assay; micro-PET/CT, micro positron emission tomography/computed tomography.

Experimental design

The number of tumor-bearing mice in each group was determined based on a combination of literature and statistics (17). Tumor-bearing mice were randomly divided into 4 groups, including the control group (n=12), where mice received intragastric normal saline from days 1–7 after enrollment at a rate of 0.1 mL/day. Mice in the RT alone group (n=12) underwent RT on day 7 after enrollment at a radiation dose Dt=8 gray (Gy)/1 fraction (F). Mice in the third group, namely, the cisplatin (DDPs) combination RT group (DDPs + RT group; n=12) were intraperitoneally injected once on day 6 after enrollment (DDPs 5 mg/kg), and received RT on day 7 (Dt=8 Gy/1 F). The fourth group was the APA (molecular formula: $C_{24}H_{23}N_{5O}.CH_4SO_3$; molecular weight: 493.58. 250 mg/tablet; Hengrui Pharmaceutical Co., Ltd., Jiangsu, China) combined with RT group (APA + RT group; n=12). First, APA solution was dissolved in sterile normal saline (concentration: 40 mg/mL). Next, intragastric administration was conducted from days 1 to 7 after enrollment at 200 mg/kg/day, and a radiation dose Dt=8 Gy/1 F was administered 2 hours after completion of intragastric administration on day 7. The RT equipment included a linear accelerator (Elekta, Stockholm, Sweden), with an energy of 6 MV X-ray, and a distance of l00 cm from the skin. The research design and route are shown in *Figure 1*.

Research assessment

Micro-positron emission tomography/computed tomography

On the second day after intervention in each group, 6 tumor-bearing mice were randomly selected from each group for micro 18F-fluorodexyglucose (18F-FDG) positron emission tomography/computed tomography (micro-PET/CT; Siemens, Erlangen, Germany) examination. At 1 day after administration, the mice were fasted to avoid asphyxia caused by gastric reflux during PET/CT. The same day, at 8:00 pm, the mice were anesthetized using an intraperitoneal injection of 1% sodium pentobarbital (5 mL/kg). A dose of 150–300 μCi 18F-FDG was injected through the tail vein and fixed,

and PET/CT scanning was conducted on the second day. Micro-PET/CT images were assessed by experienced nuclear medicine physicians, and the regions of interest (ROIs) at all levels of the transplanted tumor were delineated. The maximum standard uptake values (SUV_{max}) of tumors within the ROIs were calculated using computer analysis. The differences in the SUV_{max} ratio among groups were calculated as:

$$Ratio(\%) = \frac{Rate\ of\ Experimental\ Group - Rate\ of\ Reference\ Group}{Rate\ of\ Reference\ Group} \times 100\% \quad [1]$$

The 6 tumor-bearing mice in each group that underwent micro-PET/CT scanning were euthanized via cervical dislocation. Next, the tumor samples were collected, and the protein expression of VEGFR-2, CD31, Ki-67, andγ-H2AX levels were determined using immunohistochemistry (IHC). Additionally, cellular apoptosis was determined using a terminal deoxynucleotidyl transferase (TdT)-mediated deoxyuridine triphosphate (dUTP) nick-end labeling (TUNEL) apoptosis assay kit.

Tumor growth inhibition rate (TGIR) and survival

In addition to the 6 tumor-bearing mice that underwent the micro-PET/CT scan, the TGIR and survival of the additional mice in each group were observed. The maximum diameter (d_{max}) and minimum diameter (d_{min}) of tumors in each group was measured using a vernier caliper every 2 days starting from the first day post-administration until the 25th day. The mean tumor volumes (TVs) were calculated using $TVs = d_{max} \times d_{min}^2/2$ and TGIR was calculated using $TGIR\ (\%) = (Reference\ Group\ TVs - Experimental\ Group\ TVs)/Reference\ Group\ TVs \times 100\%$. Survival times, which started from the first day post-administration, were observed until death. Next, the median survival period was calculated. The differences of TVs and TGIR ratio among groups were calculated using Eq. [1].

VEGFR-2

The paraffin-embedded tissues were fixed in 10% formalin and sliced into 5-μm-thick sections using a microtome (Leica Biosystems, Wetzlar, Germany). The samples were deparaffinized using xylene, rehydrated with a gradient alcohol series, and treated with 500 W microwave using 10 mM citrate buffer (pH 6.0) twice for 5 minutes each time. After rinsing in Tris-buffered saline (pH 7.6), the sections were immersed in H_2O_2 (3%) solution to block endogenous peroxidase activity. Next, 5% fetal bovine serum (FBS; 1:20) was added and the sample was mixed with a primary antibody (VEGFR-2; Bio-World, Dublin, USA) and incubated overnight at 4 ℃. The next day, the sections were washed. The first antibody (Bio-World, USA) was tested using an appropriate secondary antibody at 37 ℃ and incubated for 30 minutes in an atmosphere of CO_2 at 37 ℃ in a constant temperature incubator (Thermo Fisher Scientific, Waltham, MA, USA). Diaminobenzidine (DAB) was used for color development. Next, reverse staining was conducted using hematoxylin. Lastly, the plates were sealed, dried, and visualized using an inverted microscope (Nikon, Tokyo, Japan). The criterion of VEGFR-2 protein expression was the claybank or brown staining of the cytomembrane evaluated by 2 independent pathologists. Calculation of VEGFR-2 positive cells was performed by selecting 5 fields for each section. The number of positive cells in each field was counted under a microscope (×400), and the mean number of positive cells in the 5 fields was calculated as the number of positive cells in the section. The difference in VEGFR-2 expression ratio among groups was calculated using Eq. [1].

CD31, Ki-67, γ-H2AX

The methods and steps of CD31, Ki-67, and γ-H2AX were similar to those used for the determination of VEGFR-2, with the exception of the primary antibodies targeting CD31, Ki-67, and γ-H2AX (Bio-World, USA), respectively. The criterion of CD31-positive expression was that the CD3l-positive vascular endothelial cytoplasm was stained either claybank or brown. The criteria of Ki-67 and γ-H2AX positive protein expression were the claybank or brown staining within the nucleus. Calculation of CD31-, Ki-67-, and γ-H2AX-positive cells was similar to that used for VEGFR-2. The differences in CD31, Ki-67, and γ-H2AX expression ratio among groups were calculated using Eq. [1].

Apoptosis

Cellular apoptosis was determined using a TUNEL assay (Roche, Basel, Switzerland). Paraffin sections were dewaxed, dehydrated, washed, reacted with the TUNEL reaction mixture, incubated at 37 ℃ for 60 minutes, washed again, and then observed using fluorescence microscopy. They were also mixed with the conversion agent POD, incubated at 37 ℃ for 30 minutes, and washed again. Then, DAB substrate solution was added, the samples were incubated at room temperature for 5–20 minutes, and observed using optical microscopy. The criterion of cellular apoptosis was either the presence of claybank or brown within the nucleus

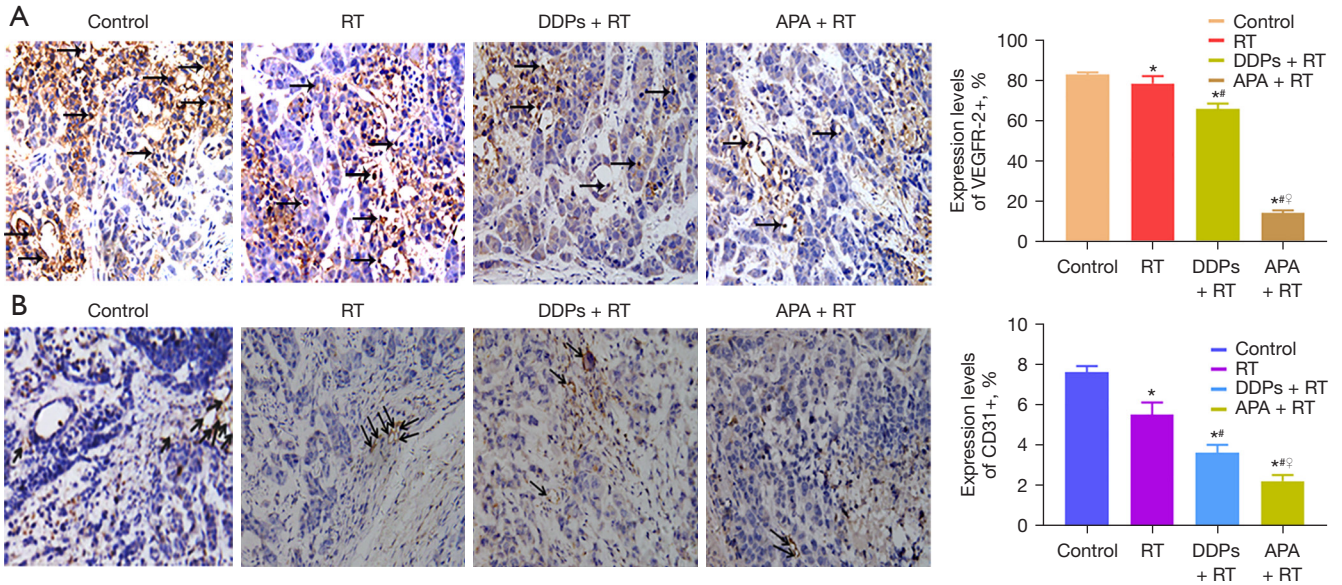

Figure 2 Protein expression of VEGFR-2 (claybank or brown in the cytomembrane, × 400, black arrows) and CD31 (claybank or brown in the nucleus, × 400, black arrows) among groups. Results from IHC and the bar chart revealed that the positive expression rates of VEGFR-2 (A) and CD31 (B) in the APA + RT group were the lowest compared with the control, RT, and DDPs + RT groups (F=84.19, 36.90, 73.59, and 27.0, 10.92, 8.38, respectively, P<0.05). *, compared with the control group; #, compared with the RT group; ♀, compared with the DDPs + RT group. RT, radiotherapy; DDPs, cisplatin; APA, apatinib; VEGFR-2, vascular endothelial growth factor receptor-2; CD31, platelet endothelial cell adhesion molecule-1; IHC, immunohistochemistry.

evaluated by 2 independent pathologists. Calculation of apoptosis was similar to those with VEGFR-2. The difference in the ratio of apoptosis levels among groups was calculated using Eq. [1].

Statistical analysis

Statistical analyses were conducted using the software SPSS 17.0 (SPSS, Inc., Chicago, IL, USA). All data were expressed as mean ± standard deviation (SD). One-way analysis of variance (ANOVA) and least significant difference (LSD)-*t* tests were used for comparisons between groups. Survival curves were fitted based on the Kaplan-Meier method, and P<0.05 was considered statistically significant.

Results

Protein expression levels of VEGFR-2 and CD31

The protein expression levels of VEGFR-2 (*Figure 2A*) and CD31 (*Figure 2B*) in the APA + RT group was significantly lower than those in the control, RT, and DDPs + RT groups (reduced by 83.4%, 82.2%, 78.8%, and 71.1%, 60.0%, 38.9%, F=84.19, 36.90, 73.59, and 27.0, 10.92, 8.38, respectively; P<0.05). The protein expression levels of VEGFR-2 and CD31 in the DDPs + RT group were lower than those in the control and RT groups (reduced by 20.8%, 16.2%, and 52.6%, 34.5%, F=7.98, 6.80, and 19.37, 9.24, respectively; P<0.05). The protein expression levels of VEGFR-2 and CD31 in the RT group were only reduced by 5.4% and 27.6% compared with the control group (t=3.00 and 12.30, respectively; P<0.05). The differences of VEGFR-2 and CD31 in the APA + RT group were most significant compared with the other groups (*Table 1*).

Protein expression levels of Ki-67, γ-H2AX, and apoptosis

The protein expression level of Ki-67 (*Figure 3A*) in the APA + RT group was lower than that in the control, RT, and DDPs + RT groups (reduced by 84.2%, 77.8%, and 65.6%, F=57.73, 24.46, and 56.99, respectively; P<0.05). The protein expression level of Ki-67 in the DDPs + RT group was lower than that in the control and RT groups (reduced by 54.1% and 35.6%, F=38.33 and 10.68, respectively;

Table 1 Comparisons of VEGFR-2, CD31, Ki-67, γ-H2AX, and apoptosis protein expression levels among groups (n=6, mean ± SD)

Groups	Rates of VEGFR-2 (ratio, %)	Rates of CD31 (ratio, %)	Rates of Ki-67 (ratio, %)	Rates of γ-H2AX (ratio, %)	Levels of apoptosis (ratio, %)
Control	82.7±1.0	7.6±0.3	93.0±3.1	5.4±0.4	5.2±0.8
RT	78.2±3.7 (–5.4$^{\downarrow}$)	5.5±0.6* (–27.6$^{\blacktriangle}$)	66.3±3.4* (–28.7$^{\blacktriangle}$)	21.4±2.0* (+296.3$^{\uparrow\blacktriangle}$)	10.3±1.5* (+98.1$^{\blacktriangle}$)
DDPs + RT	65.5±2.8 (–20.8$^{\blacktriangle}$/–16.2$^{\triangledown}$)	3.6±0.4 (–52.6$^{\blacktriangle}$/–34.5$^{\triangledown}$)	42.7±2.1 (–54.1$^{\blacktriangle}$/–35.6$^{\triangledown}$)	42.2±2.9 (+681.5$^{\blacktriangle}$/+97.2$^{\triangledown}$)	22.7±3.0 (+336.5$^{\blacktriangle}$/+120.4$^{\triangledown}$)
APA + RT	13.9±1.3*$^{\#\varphi}$ (–83.4$^{\blacktriangle}$/–82.2$^{\triangledown}$/–78.8$^{\triangle}$)	2.2±0.3*$^{\#\varphi}$ (–71.1$^{\blacktriangle}$/–60.0$^{\triangledown}$/–38.9$^{\triangle}$)	14.7±2.0*$^{\#\varphi}$ (–84.2$^{\blacktriangle}$/–77.8$^{\triangledown}$/–65.6$^{\triangle}$)	35.4±3.0*$^{\#\varphi}$ (+553.7$^{\blacktriangle}$/+65.4$^{\triangledown}$/–16.1$^{\triangle}$)	27.4±2.4*$^{\#\varphi}$ (+426.9$^{\blacktriangle}$/+166.0$^{\triangledown}$/+20.7$^{\triangle}$)

$^{\blacktriangle}$, ratio compared with control group; $^{\triangledown}$, ratio compared with RT group; $^{\triangle}$, ratio compared with DDPs + RT group; $^{\uparrow}$, increasing; $^{\downarrow}$, decreasing; *, P value compared with control group (P<0.05); $^{\#}$, P value compared with RT group (P<0.05); $^{\varphi}$, P value compared with DDPs + RT group (P<0.05). VEGFR-2, vascular endothelial growth factor receptor; CD31, platelet endothelial cell adhesion molecule-1; Ki-67, proliferating cell nuclear antigen; γ-H2AX, Histone H2AX family member; RT, radiotherapy; DDPs, cisplatin; APA, apatinib.

P<0.05). The protein expression level of Ki-67 in the RT group was lower than that in the control group (reduced by 28.7%; t=11.88, P<0.05). The difference of Ki-67 in the APA + RT group was most significant compared with the other groups (*Table 1*).

The protein expression levels of γ-H2AX (*Figure 3B*) and the apoptotic rate of tumor cells (*Figure 3C*) in the APA + RT group were higher than those in the control and RT groups (increased by 553.7%, 65.4% and 426.9%, and 166.0%, F=22.18, 23.15, and 30.86, 20.51, respectively, P<0.05). The protein expression of γ-H2AX in the APA + RT group was reduced by 16.1% (t=7.36, P<0.05), whereas the apoptosis rate was increased by 20.7% (t=2.75, P=0.04) compared with the DDPs + RT group. The protein expression levels of γ-H2AX and apoptosis in the DDPs + RT group were higher than those in the control and RT groups (increased by 681.5%, 97.2% and 336.5%, 120.4%, F=28.50, 38.16 and 13.01, 11.60, respectively, P<0.05). The protein expression levels of γ-H2AX and apoptosis in the RT group were higher than those in the control group (increased by 296.3% and 98.1%, t=17.35 and 9.65, respectively, P<0.05). The differences of γ-H2AX and apoptosis in the APA + RT group were most significant compared with the other groups (*Table 1*).

Tumor volume, TGIR, SUVmax, and survival

Starting from the fifth day post-treatment, tumor growth within the APA + RT group was significantly reduced compared with the control and RT groups. The tumor volume (*Figure 4A*) in the APA + RT group was lower than that in the control and RT groups (reduced by 49.4% and 27.4%; F=3.97 and 4.77, respectively, P<0.05). There were no significant differences in tumor volume between the APA + RT and DDPs + RT groups (only reduced by 5.3%; t=1.97, P>0.05). However, the tumor volume in the RT and DDPs + RT groups was lower compared with the control group (reduced by 30.3% and 46.6%; t=3.50 and 4.13, respectively, P<0.05). The tumor volume in the DDPs + RT group was lower compared with the RT group (reduced by 23.3%; t=5.55, P<0.05). The TGIR in the APA + RT group was higher compared with the RT and DDPs + RT groups, as it was increased by 63.8% and 25.6%, respectively (P<0.05), whereas TGIR in the DDPs + RT group was increased by 21.8% compared with the RT group (P<0.05). Hence, the differences of tumor volume and TGIR in the APA + RT group were most significant compared with the other groups (*Table 2*).

The SUV_{max} (*Figure 4B,4C*) in the APA + RT group was lower compared with the control, RT, and DDPs + RT groups (reduced by 53.1%, 42.3%, and 21.1%; F=15.25, 15.11, and 7.73, respectively, P<0.05). Furthermore, SUV_{max} in the RT and DDPs + RT groups was lower compared with the control group (reduced by 18.8% and 40.6%; t=3.70 and 15.25, respectively, P<0.05). Additionally, the SUV_{max} in the DDPs + RT group was lower compared with the RT group (reduced by 26.9%; t=13.39, P<0.05). The length of survival (*Figure 4D*) was longer by 22 and 11 days in the APA + RT group compared with the RT and DDPs + RT groups (P<0.05). Thus, the differences in the SUV_{max} and median survival in the APA + RT group were most significant compared with the other groups (*Table 2*).

Discussion

There are a few reports regarding the use of anti-

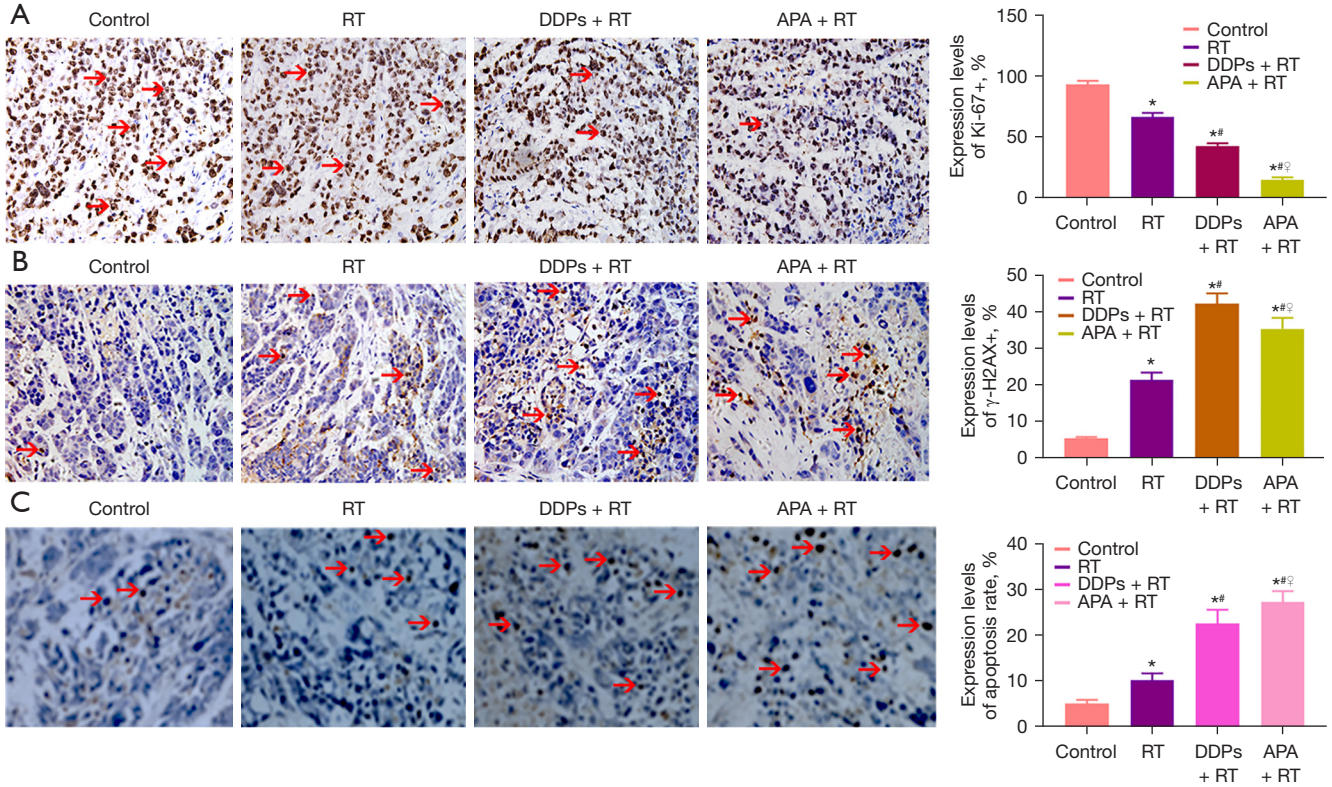

Figure 3 Protein expressions of Ki-67, γ-H2AX and apoptosis (×400, red arrows, claybank or brown in the nucleus) among groups. Results from IHC and the bar chart revealed that the positive expression rate of Ki-67 (A) in the APA + RT group was lowest compared with the control, RT, and DDPs + RT groups (F=57.73, 24.46 and 56.99, respectively, P<0.05). The positive expression rate of γ-H2AX (B) in the APA + RT group was higher compared with the control and RT groups (F=22.18 and 23.15, respectively, P<0.05), but was lower compared with the DDPs + RT group (t=7.36, P<0.05). The apoptosis rate (C) in the APA + RT group was the highest compared with the control, RT, and DDPs + RT groups (F=30.86, 20.51, and 2.75, respectively, P<0.05). *, compared with the control group; #, compared with the RT group; ♀, compared with the DDPs + RT group. RT, radiotherapy; DDPs, cisplatin; APA, apatinib; Ki-67, proliferating cell nuclear antigen; γ-H2AX, histone H2AX family member; IHC, immunohistochemistry.

angiogenesis therapy in the treatment of cervical cancer. Bevacizumab, which is primarily used in combination with chemotherapy (18,19), reduces the risk of death (0.536. 95% CI: 0.32 to 0.905; P=0.0196) and prolongs median OS by 5.8 months among patients with cervical cancer (19). The novel and highly selective VEGFR-2 tyrosine kinase inhibitor, APA, has been shown to be efficacious and safe in the treatment of advanced gastric cancer (11). Furthermore, there has been a lack of research on APA combination RT in cervical cancer. Herein, we demonstrated that the expression of VEGFR-2 and neovascularization with in the APA + RT group was significantly lower compared with the RT and DDPs + RT groups (reduced by 82.2% and 78.8%, 60.0% and 38.9%, respectively; P<0.05). When combined with RT, APA could further reduce 66.0% and 24.5% of VEGFR-2 and CD31 expression compared with the DDPs + RT group, respectively. These results suggested that APA combined with RT could significantly enhance the inhibition of VEGFR-2, decrease the expression of CD31, and reduce tumor angiogenesis. The reasons might be attributed to the effect of RT on the vascular endothelial cells in addition to the anti-angiogenic effect of APA. The combination of APA and RT might have a synergistic effect on anti-tumor angiogenesis.

The main objective of radiation is to induce DNA double-strand breaks in tumor cells (20). The results from this study demonstrated that phospho-H2AX or γ-H2AX, a biomarker for DNA double-strand breakage, can be used for DNA repair detection post-radiation (21). A study on the use of camptothecin derivative (TLC388) on H23

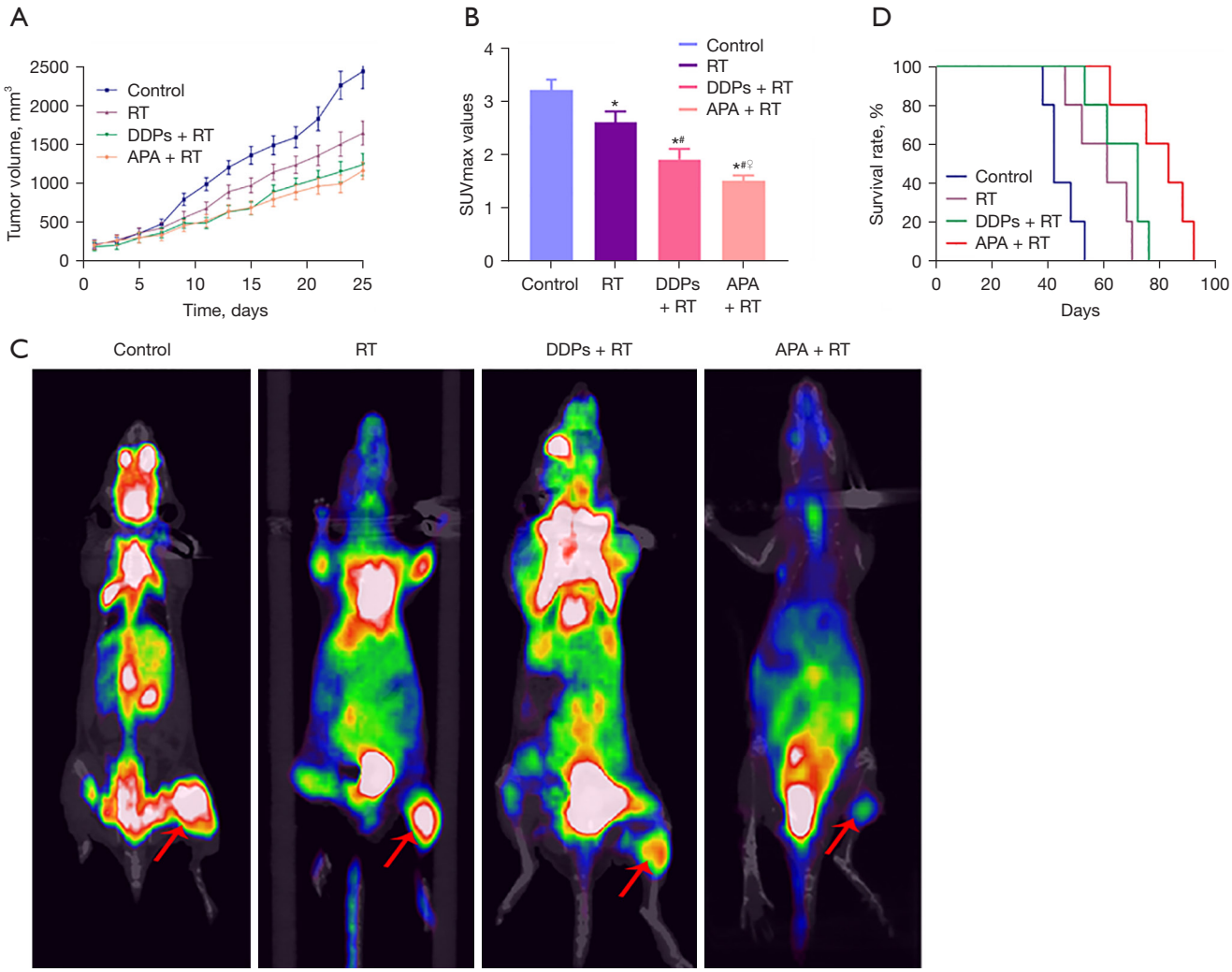

Figure 4 Tumor volume and metabolism, and survival among groups. Results from the curve and the bar chart, and micro-PET/CT (red arrows) revealed that the tumor volume (A) in the APA + RT group was significantly lower compared with the control and RT groups (F=3.97 and 4.77, respectively, P<0.05). Tumor metabolism (B,C) in the APA + RT group was significantly lower compared with the control, RT, and DDPs + RT groups (F=15.25, 15.11, and 7.73, respectively, P<0.05). The median survival (D) in the APA + RT group was longer by 22 and 11 days compared with the RT and DDPs + RT groups (P<0.05), respectively. *, compared with the control group; #, compared with the RT group; ♀, compared with the DDPs + RT group. RT, radiotherapy; DDPs, cisplatin, APA, apatinib; microPET/CT, micro positron emission tomography/computed tomography.

human non-small cell lung cancer cells revealed that the combination therapy of TLC388 and RT significantly increased γ-H2AX foci percentage (65.4% *vs.* 26.1%) compared with that using RT alone (22). Results from our study demonstrated that the levels of γ-H2AX foci in the APA + RT group were significantly higher compared with the RT group as it increased by 65.4% (P<0.05), but was lower compared with the DDPs + RT group (reduced by 16.1%). The results of our study suggested that APA combined with RT could significantly enhance DNA double-strand breaks. In addition to the direct damage of radiation to DNA, the anti-angiogenesis effect of APA might have also resulted in double-strand breaks in DNA, indicating that APA combined with RT could have a synergistic effect in enhancing double-strand breaks in DNA.

Table 2 Comparisons of tumor volume, TGIR, SUVmax, and median survival among groups (n=6)

Groups	Tumor volume (mm^3, mean ± SD) (ratio, %)	TGIR (ratio, %)	SUV_{max} (mean ± SD) (ratio, %)	Median survival (days)
Control	1,234.0±859.3		3.2±0.2	42
RT	859.1±489.2* (–30.3$^{\downarrow}$)	34.8	2.6±0.2* (–18.8$^{\blacktriangle}$)	61*
DDPs + RT	658.8±365.9*$^{\#}$ (–46.6$^{\blacktriangle}$/–23.3$^{\triangledown}$)	42.4$^{\#}$ (+21.8$^{\uparrow}$)	1.9±0.2*$^{\#}$ (–40.6$^{\blacktriangle}$/–26.9$^{\triangledown}$)	72*$^{\#}$
APA + RT	623.9±313.2*$^{\#}$ (–49.4$^{\blacktriangle}$/–27.4$^{\triangledown}$/–5.3$^{\triangle}$)	57.0$^{\#\varphi}$ (+63.8$^{\triangledown}$/+25.6$^{\triangle}$)	1.5±0.1*$^{\#\varphi}$ (–53.1$^{\blacktriangle}$/–42.3$^{\triangledown}$/–21.1$^{\triangle}$)	83*$^{\#\varphi}$

*, P value compared with control group (P<0.05); $^{\#}$, P value compared with RT group (P<0.05); $^{\varphi}$, P value compared with DDPs + RT group (P<0.05); $^{\uparrow}$, increasing; $^{\downarrow}$, decreasing; $^{\blacktriangle}$, ratio compared with control group; $^{\triangledown}$, ratio compared with RT group; $^{\triangle}$, ratio compared with DDPs + RT group. TGIR, tumor growth inhibition rate; SUV_{max}, the maximum standard uptake value; RT, radiotherapy; DDPs, cisplatin; APA, apatinib.

The expression of Ki-67, an antigen associated with cell proliferation, is closely related to tumor prognosis. A study of patients with breast cancer demonstrated that the expression of Ki-67 ≥14% significantly increased recurrence and was associated with shorter OS (23). Our study demonstrated that the expression of Ki-67 in the APA + RT group was significantly lower compared with the control, RT, and DDPs + RT groups. In combination with RT, APA could further reduce 42.2% of Ki-67 levels compared with the DDPs + RT group. Our results demonstrated that APA combined with RT could significantly reduce Ki-67 expression in tumor cells, and tumor cell proliferation activity post-radiation of cervical cancer. The reason was likely mainly attributable to the increase in DNA double strand breaks.

Apoptosis is the main method of radiation-induced tumor cell death (24). A study has demonstrated that VEGFR-2 is closely related to apoptosis, and that the inhibition of VEGFR-2 can significantly increase the extent of apoptosis (25). Our study demonstrated that the extent of apoptosis in tumor cells within the APA + RT group was significantly higher compared with the control, RT, and DDPs + RT groups. In combination with RT, APA could further increase apoptosis by 45.6% compared with the DDPs + RT group. These results were consistent with VEGFR-2 expression. This indicated that APA combined with RT could significantly increase apoptosis of tumor cells after radiation of cervical cancer, which was likely related to the inhibition of VEGFR-2 and the increase in DNA double-strand breaks.

The method of PET/CT scanning is commonly used to evaluate tumor tissue metabolism, and SUV_{max} is an important evaluation parameter (26-28). In a study that evaluated PET/CT scanning as a predictor of survival among 92 patients with bone or soft tissue tumors, researchers used SUV_{max} =10.8 as a cut-off. All patients were divided into 2 groups based on whether they were above or below the cut-off value. The median follow-up period was 2.8 years with a range of 0.04 to 11.2 years. The mortality rates of the 2 groups were 64.4% (29/45) and 25.5% (12/47), respectively. The probabilities of the 5-years survival were 29.0% and 71.0%, while the average survival was 3.1 years (95% CI: 2.2 to 4.0 years) and 8.6 years (95% CI: 7.3 to 9.8 years) (25). A study using PET/CT within invasive cervical squamous cell carcinoma has demonstrated that SUV value is an independent risk factor associated with tumor recurrence and closely related to progression-free survival (29). Results from the clinicopathological data of uterine carcinosarcoma suggest that glycolysis and metabolic tumor volume, seen on PET/CT scanning, are significantly related to tumor recurrence. In addition, the higher the glycolysis and metabolic tumor volume, the higher the risk of tumor recurrence (30).

Our study demonstrated that SUV_{max} and tumor volume within the APA + RT group were significantly lower compared with the control, RT, and DDPs + RT groups (P<0.05). In addition, the tumor growth inhibition rate within the APA + RT group was significantly higher compared with the RT and DDPs + RT groups (P<0.05). The median survival in the APA + RT group was prolonged by 22 and 11 days compared with the RT and DDPs + RT groups, respectively (P<0.05). Our results indicated that APA combined with RT could significantly reduce the SUV_{max} value and tumor volume, and prolong the median survival in an *in vivo* model of cervical cancer. The possible mechanisms of APA combined with RT are shown in *Figure 5*.

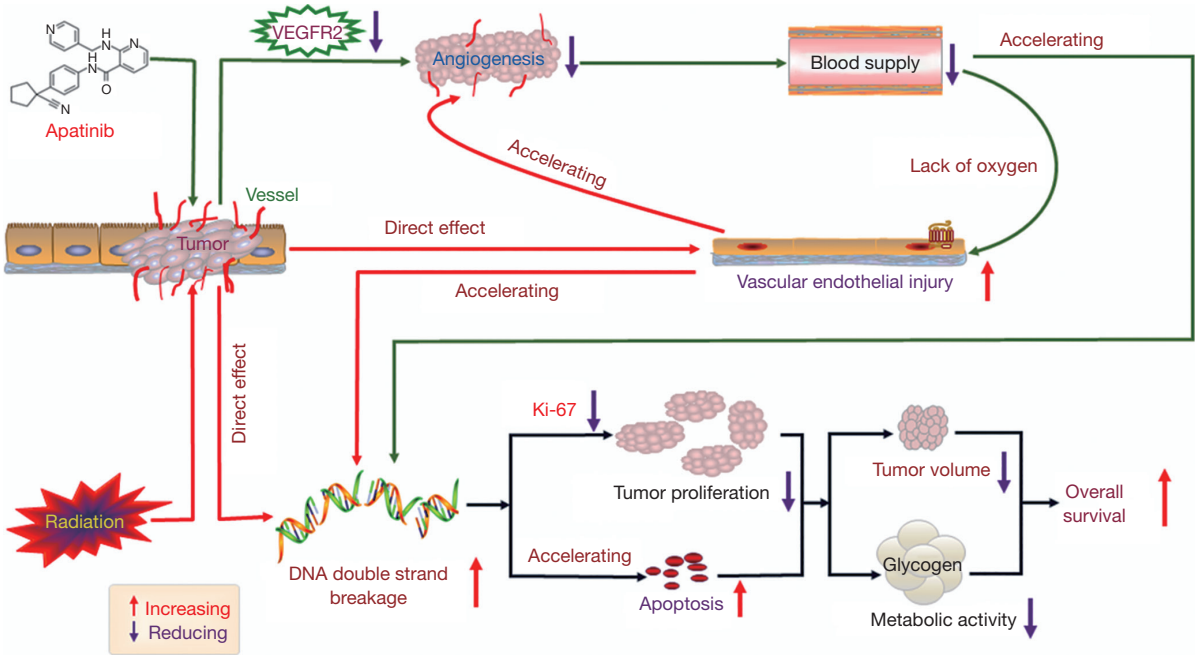

Figure 5 The possible mechanisms of APA combined with RT. There were synergistic effects on anti-tumor angiogenesis, DNA double-strand breaks, when APA combined with radiation, which resulted in reducing tumor proliferative activity by decreased Ki-67 expression, and increasing of apoptosis in tumor cell, this in turn leaded to tumor shrinkage and decreased metabolic activity. The green was mainly mechanisms of APA. The red was mainly mechanisms of RT. The bluish-gray was combined effects of APA combined with RT. Ki-67, proliferating cell nuclear antigen; APA, apatinib; RT, radiotherapy.

Conclusions

In this study, we used an *in vivo* model of cervical cancer, and demonstrated that APA combined with RT could significantly enhance the anti-tumor effect of radiation, and extend median survival. In addition to inhibition of VEGFR-2, the combination treatment could significantly enhance DNA double-strand breakage, lower the expression of CD31 and Ki-67, and enhance apoptosis. However, the relationship between APA and VEGFR-2 inhibition remains to be further studied. We used HeLa cells in this study, which is not a cervical squamous cell cancer cell line; thus, this is a limitation of our study.

Acknowledgments

We thank the programs for the funds provided, as well as the Oncology Department and Central Laboratory of the Affiliated Hospital of Southwest Medical University for providing us assistance.
Funding: This study was supported by the Open Program of Nuclear Medicine and Molecular Imaging Key Laboratory of Sichuan Province (HYX18017) and the Union Cancer Research Fund from the Chinese Society of Clinical Oncology (CSCO)-Hengrui (Y-HR2016-046).

Footnote

Reporting Checklist: The authors have completed the ARRIVE reporting checklist. Available at https://atm.amegroups.com/article/view/10.21037/atm-22-1442/rc

Data Sharing Statement: Available at https://atm.amegroups.com/article/view/10.21037/atm-22-1442/dss

Conflicts of Interest: All authors have completed the ICMJE uniform disclosure form (available at https://atm.amegroups.com/article/view/10.21037/atm-22-1442/coif). The authors have no conflicts of interest to declare.

Ethical Statement: The authors are accountable for all aspects of the work in ensuring that questions related to the accuracy or integrity of any part of the work are

appropriately investigated and resolved. Experiments were performed under a project license (No. swum20210388) granted by the Institutional Animal Care and Treatment Committee of Southwest Medical University, in compliance with China national guidelines for the care and use of animals.

References

1. Cohen PA, Jhingran A, Oaknin A, et al. Cervical cancer. Lancet 2019;393:169-82.
2. Jung KW, Won YJ, Kong HJ, et al. Cancer Statistics in Korea: Incidence, Mortality, Survival, and Prevalence in 2016. Cancer Res Treat 2019;51:417-30.
3. Feng RM, Zong YN, Cao SM, et al. Current cancer situation in China: good or bad news from the 2018 Global Cancer Statistics? Cancer Commun (Lond) 2019;39:22.
4. Cao W, Chen HD, Yu YW, et al. Changing profiles of cancer burden worldwide and in China: a secondary analysis of the global cancer statistics 2020. Chin Med J (Engl) 2021;134:783-91.
5. Sakuragi N, Kaneuchi M, Kato T, et al. Tailored radical hysterectomy for locally advanced cervical cancer. Int J Gynecol Cancer 2020;30:1136-42.
6. Sakuragi N, Kato T, Shimada C, et al. Oncological Outcomes After Okabayashi-Kobayashi Radical Hysterectomy for Early and Locally Advanced Cervical Cancer. JAMA Netw Open 2020;3:e204307.
7. Matsuo K, Machida H, Mandelbaum RS, et al. Validation of the 2018 FIGO cervical cancer staging system. Gynecol Oncol 2019;152:87-93.
8. Wright JD, Matsuo K, Huang Y, et al. Prognostic Performance of the 2018 International Federation of Gynecology and Obstetrics Cervical Cancer Staging Guidelines. Obstet Gynecol 2019;134:49-57.
9. Lee J, Lin JB, Sun FJ, et al. Safety and efficacy of semiextended field intensity-modulated radiation therapy and concurrent cisplatin in locally advanced cervical cancer patients: An observational study of 10-year experience. Medicine (Baltimore) 2017;96:e6158.
10. Mori T, Makino H, Okubo T, et al. Multi-institutional phase II study of neoadjuvant irinotecan and nedaplatin followed by radical hysterectomy and the adjuvant chemotherapy for locally advanced, bulky uterine cervical cancer: A Kansai Clinical Oncology Group study (KCOG-G1201). J Obstet Gynaecol Res 2019;45:671-8.
11. Zhao TT, Xu H, Xu HM, et al. The efficacy and safety of targeted therapy with or without chemotherapy in advanced gastric cancer treatment: a network meta-analysis of well-designed randomized controlled trials. Gastric Cancer 2018;21:361-71.
12. Yu WC, Zhang KZ, Chen SG, et al. Efficacy and Safety of apatinib in patients with intermediate/advanced hepatocellular carcinoma: A prospective observation study. Medicine (Baltimore) 2018;97:e9704.
13. Zhao C, Zhang Q, Qiao W. Significant efficacy and well safety of apatinib combined with radiotherapy in NSCLC: Case report. Medicine (Baltimore) 2017;96:e9276.
14. Zhao F, Tian W, Zeng M, et al. Apatinib alone or combined with radiotherapy in metastatic prostate cancer: Results from a pilot, multicenter study. Oncotarget 2017;8:110774-84.
15. Guo Q, Sun Y, Kong E, et al. Apatinib combined with chemotherapy or concurrent chemo-brachytherapy in patients with recurrent or advanced cervical cancer: A phase 2, randomized controlled, prospective study. Medicine (Baltimore) 2020;99:e19372.
16. Zhou JG, Zhou NJ, Zhang Q, et al. Apatinib for patients with advanced or recurrent cervical cancer: study protocol for an open-label randomized controlled trial. Trials 2018;19:500.
17. Qin RS, Zhang ZH, Zhu NP, et al. Enhanced antitumor and anti-angiogenic effects of metronomic Vinorelbine combined with Endostar on Lewis lung carcinoma. BMC Cancer 2018;18:967.
18. Kumar L, Harish P, Malik PS, et al. Chemotherapy and targeted therapy in the management of cervical cancer. Curr Probl Cancer 2018;42:120-8.
19. Tewari KS, Sill MW, Monk BJ, et al. Prospective Validation of Pooled Prognostic Factors in Women with Advanced Cervical Cancer Treated with Chemotherapy with/without Bevacizumab: NRG Oncology/GOG Study. Clin Cancer Res 2015;21:5480-7.
20. Bannik K, Madas B, Jarke S, et al. DNA repair inhibitors sensitize cells differently to high and low LET radiation. Sci Rep 2021;11:23257.

21. Raavi V, Perumal V, Paul SFD. Potential application of gamma-H2AX as a biodosimetry tool for radiation triage. Mutat Res Rev Mutat Res 2021;787:108350.
22. Storozynsky Q, Hitt MM. The Impact of Radiation-Induced DNA Damage on cGAS-STING-Mediated Immune Responses to Cancer. Int J Mol Sci 2020;21:8877.
23. Tay TKY, Thike AA, Pathmanathan N, et al. Using computer assisted image analysis to determine the optimal Ki67 threshold for predicting outcome of invasive breast cancer. Oncotarget 2018;9:11619-30.
24. Li MY, Liu JQ, Chen DP, et al. Radiotherapy induces cell cycle arrest and cell apoptosis in nasopharyngeal carcinoma via the ATM and Smad pathways. Cancer Biol Ther 2017;18:681-93.
25. Peng H, Zhang Q, Li J, et al. Apatinib inhibits VEGF signaling and promotes apoptosis in intrahepatic cholangiocarcinoma. Oncotarget 2016;7:17220-9.
26. Shibasaki M, Iwai T, Oguri S, et al. Role of 18F-fluorodeoxyglucose positron emission tomography/computed tomography in predicting pathological response to preoperative super-selective intra-arterial chemoradiotherapy for advanced squamous cell carcinoma of the mandible. J Bone Oncol 2018;11:33-7.
27. Andersen KF, Fuglo HM, Rasmussen SH, et al. Semi-Quantitative Calculations of Primary Tumor Metabolic Activity Using F-18 FDG PET/CT as a Predictor of Survival in 92 Patients With High-Grade Bone or Soft Tissue Sarcoma. Medicine (Baltimore) 2015;94:e1142.
28. Kaira K, Higuchi T, Naruse I, et al. Metabolic activity by 18F-FDG-PET/CT is predictive of early response after nivolumab in previously treated NSCLC. Eur J Nucl Med Mol Imaging 2018;45:56-66.
29. Chung HH, Cheon GJ, Kim JW, et al. Prognostic importance of lymph node-to-primary tumor standardized uptake value ratio in invasive squamous cell carcinoma of uterine cervix. Eur J Nucl Med Mol Imaging 2017;44:1862-9.
30. Lee JW, Heo EJ, Moon SH, et al. Prognostic value of total lesion glycolysis on preoperative 18F-FDG PET/CT in patients with uterine carcinosarcoma. Eur Radiol 2016;26:4148-54.

Cite this article as: Wang Y, Zhang L, Liu W, Yang JP, Peng HJ, Zhang JW. Apatinib enhances the antitumor effects of radiation in HeLa cell line mouse model of invasive cervical cancer. Ann Transl Med 2022;10(8):459. doi: 10.21037/atm-22-1442